Research Article | Vol. 29, No. 8 / 12 April 2021 / Optics Express 12736
Optics EXPRESS

Multifunctional ultrathin reflective metasurface via polarization-decoupled phase for arbitrary circularly or elliptically polarized waves

XIAOYUAN HE,[1] LI DENG,[1,*] YANG YANG,[2] AND BOTAO FENG[3]

[1]*Beijing Laboratory of Advanced Information Networks and Beijing Key Laboratory of Network System Architecture and Convergence, Beijing University of Posts and Telecommunications, Beijing 100876, China*
[2]*Tech Lab, School of Electrical and Data Engineering, University of Technology Sydney, Botany, NSW 2019, Australia*
[3]*College of Electronics and Information Engineering, Shenzhen University, Shenzhen 518060, China*
[*]*dengl@bupt.edu.cn*

Abstract: Metasurface offers a promising platform in the design of multifunctional devices owing to its unique ability for EMWs manipulation. However, wave-manipulation capabilities for metasurfaces face challenges in manipulating orthogonal EMWs with arbitrary circularly or elliptically polarized EMWs in the microwave region. Herein, single-layer reflective metasurfaces are proposed for independent manipulation of an arbitrary set of orthogonal circularly or elliptically polarized EMWs via polarization-decoupled phase. Taking advantage of single-layer anisotropic meta-atoms, the proposed metasurface can act as a tandem phase modulator, which introduces polarization-decoupled phase profiles for arbitrary circularly and elliptically polarized EMWs based on the Jones matrix. In this way, the proposed metasurface can distinguish a set of orthogonal EMWs with circular or elliptical polarization states and impose arbitrary phase profiles on them independently and simultaneously. For proof-of-concept, bifunctional metasurfaces operating in the microwave region are presented for independent manipulation of three different sets of orthogonal circularly or elliptically polarized EMWs. They create dual independent channels associated with a pair of orthogonal polarization states, performing functions including polarization beam splitting and orbital angular momentum (OAM) multiplexing. Measured and simulated results show a good agreement, confirming that the proposed single-layer reflective metasurfaces are efficient devices that enable meta-devices to independently control arbitrary circular and elliptical polarized EMWs, achieving arbitrary functionalities.

1. Introduction

With the rapid development of modern miniaturized and integrated systems, multi-functional devices are desirable in various applications [1–3]. Metasurfaces [4–7] are ideal for multi-functional devices due to their unique ability for tailoring electromagnetic waves (EMWs) manipulation within the critical feature of ultrathin profile. Metasurfaces can control the key properties of the EMWs, such as amplitude [8,9], phase [10,11], and polarization states [12,13] by imparting amplitude or phase abruption on incidence through an interface with subwavelength thickness [14,15].

When it comes to multi-functions, one of the most representatives is the polarization-based metasurface. They use the additional degree of freedom provided by the polarization states of EMWs to create multiple polarization-dependent channels and then achieve multiple functionalities without involving additional devices. Hence, polarization manipulation plays a significant role in the design of polarization-based multi-functional metasurfaces. To date, metasurfaces based on dynamical phase [16–19] and geometric phase [11,20,21] are used to manipulate linearly and circularly polarized EMWs, respectively. However, neither of them can

#422664 https://doi.org/10.1364/OE.422664
Journal © 2021 Received 16 Feb 2021; revised 1 Apr 2021; accepted 2 Apr 2021; published 9 Apr 2021

Optics EXPRESS

independently control orthogonal EMWs with arbitrary circular or elliptical polarization states. For the independent manipulation of circular polarization states, hybrid metasurfaces based on the geometric phase were proposed to obtain helicity-independent phase engineering [22–24]. These hybrid metasurfaces are composed of two kinds of meta-atoms arranged in different layers or different segments, one of which can manipulate right-handed circularly polarized (RCP) EMWs without interfering with left-handed circularly polarized (LCP) EMWs, while the other exhibits phase response to LCP EMWs, or vice versa. In this way, independent manipulation of a pair of orthogonal circularly polarized EMWs can be achieved via a single metasurface. However, they suffer from inevitable mutual interference as they simply combine two metasurfaces that work for LCP and RCP EMWs respectively into a single one. Therefore, a more efficient method is needed for independent polarization manipulation.

Jones matrix is regarded as a powerful analytical model in the design of metasurfaces for polarization manipulation. This model unifies two categories, including dynamical phase designs and geometric phase designs, that were originally used in designing metasurfaces imparting polarization-dependent phase profiles [25]. In this way, metasurfaces can achieve complete manipulation of polarization and phase. More specifically, Jones matrix model has two operation scenarios [26,27]. On the one hand, it can help metasurfaces achieve complete control of phase and polarization of the reflective or transmissive EMWs. On the other hand, it enables metasurfaces to impart arbitrary phase profiles on a pair of orthogonal EMWs with arbitrary polarization states independently [28,29]. For example, Jones matrix is employed to obtain hybrid phase involving the dynamical phase and the geometric phase simultaneously via a single metasurface to achieve independent control of orthogonal circularly polarized EMWs [30–32]. In this way, the metasurfaces can distinguish dual-helicity EMWs and impose independent phase profiles on them. Nevertheless, they are composed of more than two dielectric substrates for the sake of the metasurface efficiency and the required helicity-decoupled phase. More importantly, both cannot build a bridge between metasurface and elliptically polarized EMWs, and so, an arbitrary set of orthogonal EMWs with elliptical polarization states cannot be recognized and independently controlled by these metasurfaces. Elliptically polarized EMWs are the most general EMWs [29]. Like linearly and circularly polarized EMWs, elliptically polarized EMWs also play an important role in providing an unprecedented degree of freedom for polarization-dependent switchable functionalities [32]. Therefore, it is of great importance to introduce polarization-decoupled phases to control orthogonal elliptically polarized EMWs independently.

In this paper, single-layer reflective metasurfaces are proposed to perform multiple functionalities via the polarization-decoupled phase for arbitrary circularly and elliptically polarized waves. They are composed of anisotropic meta-atoms with a thickness of 3mm ($0.058\lambda_0$, λ_0=free-space wavelength at 5.8 GHz), which perform well in distinguishing a set of orthogonal linearly polarized EMWs using the dynamical phase. By analyzing the Jones matrix of a metasurface under the illumination of a set of orthogonal EMWs with arbitrary circular or elliptical polarization states, the polarization-decoupled phase can be obtained by modifying the geometric shape and angular rotation of the meta-atoms, introducing dynamical and quasi-geometric phases simultaneously. Based on this concept, the proposed metasurfaces can distinguish a set of orthogonal EMWs with arbitrary circular or elliptical polarization states and impose distinct phase profiles on them, achieving independent manipulation of EMWs with both circular and elliptical polarization states. For proof-of-concept, two kinds of bifunctional reflective metasurfaces for two representative applications in the microwave region are elaborately designed. Owing to the tandem employment of dynamical phase and quasi-geometric phase, the proposed metasurfaces own a degree of freedom provided by the orthogonal polarization states of EMWs, and thereby produce two distinct functionalities associated with the polarization states of the incidence without additional devices. More specifically, one of them acts as a polarization beam splitting metasurface, which can deflect a set of orthogonal EMWs with circular or elliptical polarization states by different

Optics EXPRESS

reflection angles based on the concept of the generalized law of reflection. The other one is the orbital angular momentum (OAM) multiplexor, which creates dual polarization-dependent channels for the generation of coaxial OAM waves possessing different topological charges (TCs). Measured results are consistent with the simulated ones, confirming that the proposed single-layer multi-functional metasurfaces can enable independent control of an arbitrary pair of orthogonal EMWs with circular or elliptical polarization states.

2. Design theory

The Jones matrix is a natural framework describing the polarization manipulation by non-image-forming instruments physically [33]. Therefore, a Jones matrix is introduced for the physical description of the working mechanism of the proposed single-layer anisotropic metasurface for the manipulation of any set of orthogonal EMWs with circular or elliptical polarization states. In general, any polarization state can be described as a sum of two orthogonally polarized EMWs with distinct amplitudes and phases. Consequently, an arbitrary set of EMWs with orthogonal polarization states, namely $|\kappa^+\rangle$ and $|\kappa^-\rangle$, can be represented as a sum of x- and y-polarized EMWs with a normalized amplitude of cosω and sinω, respectively. Then, the normalized Jones vectors $|\kappa^+\rangle$ and $|\kappa^-\rangle$ are given as

$$|\kappa^+\rangle = \begin{bmatrix} \kappa_x^+ \\ \kappa_y^+ \end{bmatrix} = \begin{bmatrix} \cos\omega \\ \sin\omega \cdot e^{i\phi} \end{bmatrix}, \tag{1}$$

and

$$|\kappa^-\rangle = \begin{bmatrix} \kappa_x^- \\ \kappa_y^- \end{bmatrix} = \begin{bmatrix} -\sin\omega \\ \cos\omega \cdot e^{i\phi} \end{bmatrix}, \tag{2}$$

where ϕ refers to the phase delay between x- and y-polarized components of $|\kappa^+\rangle$ (or $|\kappa^-\rangle$); + and – denote a pair of orthogonal polarization states. For independently controlling $|\kappa^+\rangle$ and $|\kappa^-\rangle$ by imposing distinct phase profiles independently and simultaneously, the Jones matrix of the anisotropic metasurface can be obtained

$$\begin{cases} M_H(x,y)|\kappa^+\rangle = e^{i\varphi_+(x,y)}|(\kappa^+)^*\rangle \\ M_H(x,y)|\kappa^-\rangle = e^{i\varphi_-(x,y)}|(\kappa^-)^*\rangle \end{cases}, \tag{3}$$

where $\varphi_+(x,y)$ and $\varphi_-(x,y)$ are desired phase profiles for $|\kappa^+\rangle$ and $|\kappa^-\rangle$, which are introduced by meta-atom located at point (x,y); * represents complex conjugation. Then

$$M_H(x,y) = \begin{bmatrix} e^{i\varphi_+(x,y)}(\kappa_x^+)^* & e^{i\varphi_-(x,y)}(\kappa_x^-)^* \\ e^{i\varphi_+(x,y)}(\kappa_y^+)^* & e^{i\varphi_-(x,y)}(\kappa_y^-)^* \end{bmatrix} \begin{bmatrix} \kappa_x^+ & \kappa_x^- \\ \kappa_y^+ & \kappa_y^- \end{bmatrix}^{-1}. \tag{4}$$

Since the Jones matrix shown in Eq. (4) is unitary and symmetric, it can be decomposed in terms of its eigenvectors and eigenvalues matrix as Eq. (5) based on the matrix and group theory [34].

$$\begin{aligned} M_H(x,y) &= P(x,y)\Lambda(x,y)P^{-1}(x,y) \\ &= \begin{bmatrix} \cos\theta(x,y) & -\sin\theta(x,y) \\ \sin\theta(x,y) & \cos\theta(x,y) \end{bmatrix} \begin{bmatrix} e^{i\delta_x(x,y)} & 0 \\ 0 & e^{i\delta_y(x,y)} \end{bmatrix} \begin{bmatrix} \cos\theta(x,y) & \sin\theta(x,y) \\ -\sin\theta(x,y) & \cos\theta(x,y) \end{bmatrix} \end{aligned} \tag{5}$$

Obviously, $P(x,y)$ and $P^{-1}(x,y)$ are standard 2×2 rotation matrices associated with the angles $\theta(x,y)$ and $-\theta(x,y)$, meaning a geometrical in-plane rotation by $\theta(x,y)$ and $-\theta(x,y)$; $\Lambda(x,y)$ can

Optics EXPRESS

be regarded as the Jones matrix of an anisotropic metasurface for independently controlling dual EMWs by imposing distinct phase shifts $\delta_x(x,y)$ and $\delta_y(x,y)$ on x- and y-polarized EMWs. According to Eqs. (1–(5), the anisotropic meta-atom of the proposed metasurface located at point (x,y) can be regarded as a tandem phase modulator that imposes distinct phase profiles $\delta_x(x,y)$ and $\delta_y(x,y)$ on the components of the incidence whose polarization states along x- and y-direction are rotated by $\theta(x,y)$. Specifically, phase profiles $\delta_x(x,y)$ and $\delta_y(x,y)$ can be introduced using the dynamical phase, and $\theta(x,y)$ can be regarded as the quasi-geometric phase since all the meta-atoms of the anisotropic metasurface are required to be rotated by an in-plane angle $\theta(x,y)$ in an anticlockwise direction.

From a technical perspective, the essential precondition for independent control of a pair of orthogonal EMWs with arbitrary circular or elliptical polarization states is that the meta-atoms should introduce anisotropic resonators along x- and y-directions, which can be achieved simply by a single-layer structure. In this way, the distinct phase profiles $\delta_x(x,y)$ and $\delta_y(x,y)$ can be introduced by the phase responses of the anisotropic meta-atoms for x- and y-polarized EMWs. Because of the angular rotation of meta-atoms, the distinct phase profiles $\delta_x(x,y)$ and $\delta_y(x,y)$ will be transformed into phase profiles imposed onto a set of orthogonal EMWs with arbitrary circular or elliptical polarization states expressed as Eqs. (1,2). Based on this concept, a metasurface composed of single-layer anisotropic meta-atoms is able to achieve independent manipulation of an arbitrary set of orthogonal EMWs with arbitrary circular or elliptical polarization state by employing quasi-geometric phase and dynamical phase in tandem. Figure 1(a) is the schematic view of the proposed anisotropic metasurface. As shown in Fig. 1(a), a single-layer metasurface is illuminated by a set of EMWs $|\kappa^+\rangle$ and $|\kappa^-\rangle$ with arbitrary circular or elliptical polarization state. On the basis of modifying the geometric shape and angular rotation of each anisotropic meta-atoms, according to Eq. (5), distinct polarization-decoupled phase profiles can be obtained

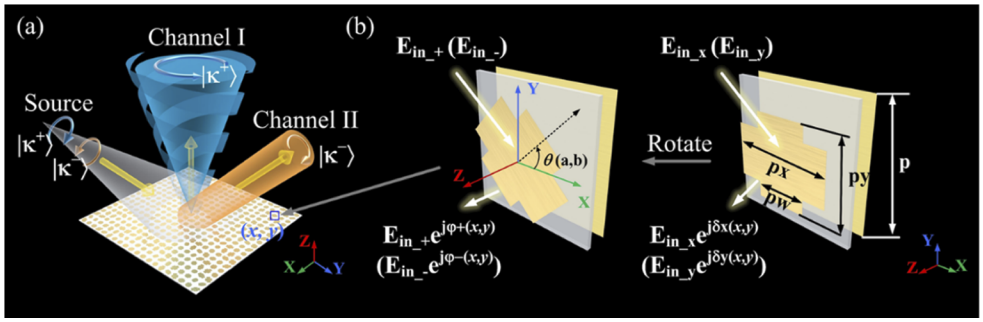

Fig. 1. (a) Schematic view of the proposed metasurface for independent manipulation of an arbitrary set of orthogonal EMWs with circular or elliptical polarization states. Illuminated by $|\kappa^+\rangle$ and $|\kappa^-\rangle$, the proposed metasurface can create dual independent channels via the polarization-decoupled phase, which is realized by modifying the geometric shape and angular rotation of the meta-atoms. (b) The conceptual design process of the proposed metasurface employing a polarization-decoupled phase. Owing to the phase-engineered ability of anisotropic meta-atoms with p=25 mm and pw=10 mm, the polarization-decoupled phase can be introduced. Two kinds of phase-engineered methods of metasurface are employed in the proposed design, one of which is also known as the dynamical phase that can be achieved by structurally varying the length of the meta-atoms px and py, enabling the independent phase control of x- and y-polarized EMWs, the other of which is called the quasi-geometric phase that can be achieved by angularly rotating the meta-atoms. In this way, the distinct phase profiles $\delta_x(x,y)$ and $\delta_y(x,y)$ will be transformed into phase profiles imposed on a set of orthogonal EMWs $|\kappa^+\rangle$ and $|\kappa^-\rangle$ with arbitrary circular or elliptical polarization states.

Optics EXPRESS

by the employment of the dynamical phase $\delta_x(x,y)$ and $\delta_y(x,y)$ and quasi-geometric phase $\theta(x,y)$. As a result, dual polarization-dependent channels can be obtained to realize versatile functionalities.

3. Single-layer metasurface with polarization-dependent functionalities

3.1. Anisotropic meta-atoms

Anisotropic meta-atoms are of great significance in the design of the proposed metasurfaces, without which a single-layer metasurface cannot be used for the independent manipulation of an arbitrary set of orthogonal EMWs with circular or elliptical polarization states. Herein, anisotropic meta-atoms operating at 5.8GHz are employed. As shown in Fig. 1(b), the anisotropic meta-atom is composed of a cross-shaped resonator, a ground plane, and an ultrathin F-4B substrate with a relative permittivity of 2.2 and a loss tangent of 0.001 between them. The thickness t of the F-4B substrate is 3mm ($0.058\lambda_0$). Owing to the cross-shaped structure, anisotropic resonances along x- and y-directions can be introduced by the meta-atoms. Thus, independent phase responses can be achieved when the incidence is with polarization states along the perpendicular lines of the cross-shaped resonator. Figures 2(a) and 2(b) show the current distributions of the anisotropic meta-atom illuminated by x- and y-polarized EMWs with an incident angle of (α=45°, β=0°) respectively, where α refers to the angle between the incidence and the + z axial; β denotes the angle between the projection of the incidence and the + x axial. Generally speaking, a metal-insulator-metal structure is an alternative method for introducing magnetic resonance, and hence dynamical phase changes can be induced [35]. As shown in Figs. 2(a) and 2(b), most currents are located parallel to the incidence polarization state. More importantly, antiparallel electric currents are created in the ground plane, introducing a magnetic mode with a strongly enhanced magnetic field inside the substrate. The magnetic mode plays an important role in the phase modulation of EMWs. More specifically, this phenomenon indicates that the phase responses of EMWs with orthogonal linear polarization states along x- and y-direction can be controlled by modifying the length of the cross-shaped resonator along the corresponding direction. Figures 2(c) and 2(d) show the reflection amplitude and phase under the illumination of x- and y-polarized EMWs with an incident angle of (α=45°, β=0°). The reflection phase of x- or y-polarized EMWs can be manipulated when the length of the cross-shaped resonator varies in x- or y-direction. Meanwhile, the reflection phases of y- or x-polarized EMWs remain nearly constant. Consequently, the anisotropic meta-atom can impose distinct phase shifts on x- and y-polarized EMWs, independently. The reflection amplitude of the meta-atoms is higher than 0.98 because of the ground plane at the bottom of the substrate, which prevents incidences from transmitting through the meta-atom.

3.2. Polarization beam splitting metasurface

For the verification of the design theory discussed above, three polarization beam splitting metasurfaces (PBSMs) are designed based on Eq. (5). Figure 3 is the conceptual diagram of the proposed PBSMs. They are designed for independent manipulation of a pair of orthogonal circularly polarized EMWs $|\kappa_1^{\pm}\rangle$ (ω_1=π/4,ϕ_1=π/2) and two different sets of elliptical polarized EMWs $|\kappa_2^{\pm}\rangle$ (ω_2=π/3,ϕ_2=π/2) and $|\kappa_3^{\pm}\rangle$ (ω_3=π/3,ϕ_3=π/4), namely PBSM #1, #2 and #3, respectively. They act as tandem phase modulators by employing the dynamical and the quasi-geometric phases, simultaneously, based on Eq. (5). Therefore, distinct phase profiles can be imposed on $|\kappa_i^{+}\rangle$ and $|\kappa_i^{-}\rangle (i = 1, 2, 3)$ independently, and dual independent channels, namely Channel I and II, can be created simultaneously. They are employed to deflect incidences in polarization-dependent directions. Assuming that the incidence $|\kappa_i^{+}\rangle$ and $|\kappa_i^{-}\rangle (i = 1, 2, 3)$ from the source located at (s_x, s_y, s_h), are deflected in the direction of (α_+=45°, β_+=90°) and (α_-=45°, β_-=270°), phase profiles

Optics EXPRESS

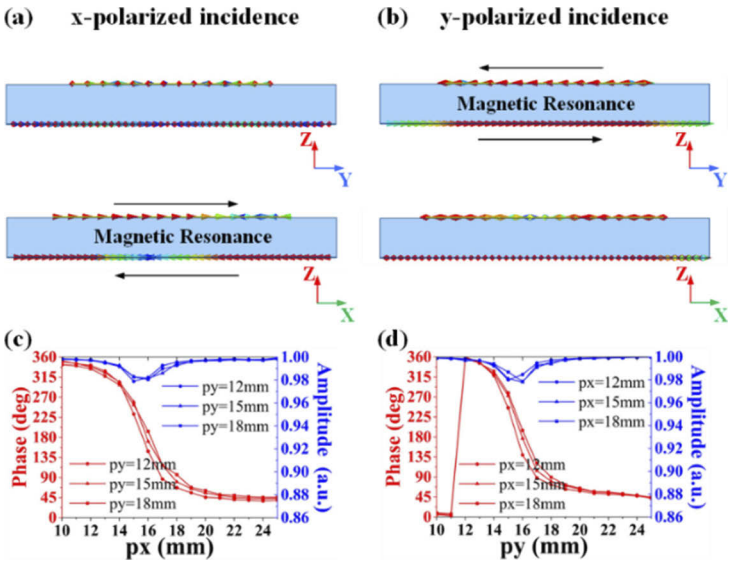

Fig. 2. Simulated current distributions of the proposed anisotropic meta-atoms under the illumination of (a)x-polarized EMWs and (b)y-polarized EMWs with an incident angle of (α=45°, β=0°). The induced currents in the cross-shaped resonator are parallel to the polarization states of incidence, and those in the ground plane are in the opposite direction. Therefore, distinct magnetic resonances can be produced by the proposed meta-atom illuminated by EMWs with x- and y-direction polarization states, indicating that the manipulation of x- and y-polarized EMWs can be independent and simultaneous. Simulated phase and amplitude responses of the proposed meta-atom under the illumination of inclined EMWs with (c)x-direction and (d)y-direction polarization states. The arbitrary reflection phase of x- and y-polarized EMWs can be achieved by modifying px or py, the length of the meta-atom along x- or y-direction. Meanwhile, the reflection phase of cross-polarized EMWs barely changes during the process.

$\varphi_+(x,y)$ and $\varphi_-(x,y)$ can be calculated according to the generalized law of reflection [2,36]

$$\varphi_\pm(x,y) = k_0 \cdot \vec{r}_\pm \cdot \vec{r}_{xy} + \varphi_s(x,y), \tag{6}$$

where $\varphi_s(x,y) = k_0\sqrt{(s_x-x)^2+(s_y-y)^2+(s_h-t)^2}$, representing the phase compensation for transforming spherical phase waves into plane waves; $\overrightarrow{r_{xy}}$ is the position vector of the meta-atom located at point (x,y); $\overrightarrow{r_+}$ and $\overrightarrow{r_-}$ are the unit vectors denoting the direction of reflected EMWs of $|\kappa_i^+\rangle$ and $|\kappa_i^-\rangle (i=1,2,3)$, respectively. Substituting in Eq. (5), the polarization-decoupled phase involving $\delta_x(x,y)$, $\delta_y(x,y)$ and $\theta(x,y)$ can be obtained for the design of the three PBSMs.

To investigate the performance of the three PBSMs, the commercial electromagnetic simulation software Computer Simulation Technology Suite (CST) was used in the simulation. Figure 4 shows the simulated results of the three PBSMs. It can be clearly observed from the far-field radiation patterns that the performances of the three PBSMs are in accordance with expected results. Under the illumination of $|\kappa_i^+\rangle (i=1,2,3)$, the reflected EMWs propagate in the direction of (α_+=45°, β_+=90°). And the incidence whose polarization state can be expressed as $|\kappa_i^-\rangle (i=1,2,3)$ are deflected in the direction of (α_-=45°, β_-=270°). Moreover, the electric-distribution on the Y-Z cutting plane was observed for further evaluation of the proposed PBSMs. The coordinate of O' is (0, 500mm, 500mm) to avoid turbulence in the near-field. And the observational plane has an area of 500 mm×500 mm. Because of the restriction of the metasurface source, only the PBSM for manipulating dual-circularly EMWs was fabricated and measured.

Optics EXPRESS

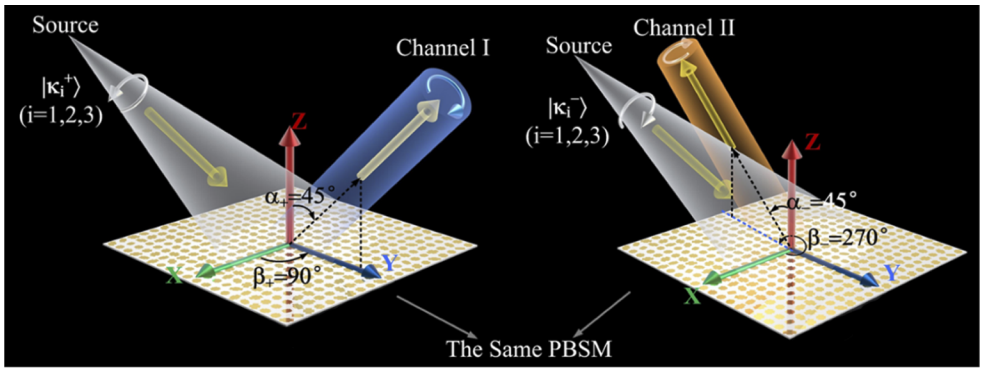

Fig. 3. Conceptual diagram of the proposed PBSMs. Based on the polarization-decoupled phase, the proposed PBSMs can create dual independent channels employed to deflect incidence with orthogonal circular or elliptical polarization states into directions depending on their polarization states.

In the experiment, a patch antenna fed by a coplanar waveguide shown in Fig. 5(a) was used to produce LCP and RCP EMWs with an incident angle (α=45°, β=0°) which is the metasurface source. As shown in Fig. 5(b), the simulated and measured reflection coefficients of the patch antenna at 5.8GHz are −20.28 and −19.63dB, respectively. The patch antenna shows LCP EMWs in the z < 0 hemispheres, while the RCP EMWs can be obtained in the z > 0 hemispheres, as shown in Figs. 5(c) and 5(d). Hence, different setups are employed to investigate the performance of PBSM #1 in both the simulation and measurement. As depicted in Fig. 6, both the metasurface and the patch antenna are fixed on the plastic apparatus, which barely affects the metasurface's performance. The patch antenna is located at (350mm, 0, 350mm). To obtain the incident EMWs with opposite helicity, the patch antenna's setup was overturned without changing its location. Figure 7(a) is the zoom-in-view photograph of the fabricated prototype. The experimental measurements of the patch antenna and PBSM #1 are conducted in an anechoic chamber, as shown in Figs. 7(b) and 7(c). The grey dashed curve in Figs. 4(a) and 4(c) are the measured results of the PBSM under the illumination of LCP and RCP EMWs. There are some defects between the simulated and measured results, which may be caused by fabrication errors of the SMA connector soldering in the feeding source. The experimental setup may also lead to the unidentical results comparing with the simulated ones. However, the main beam propagates with a reflection angle of 45° in the YOZ plane with the most considerable intensity, which shows excellent agreement with the simulated results.

In addition, the Stokes parameters of the reflected EMWs were studied to evaluate the efficiency of the proposed PBSMs further. Generally speaking, the Poincaré sphere is regarded as a convenient method for describing the polarization state of EMWs [37,38]. The Cartesian axes of the Poincaré sphere, which represent the azimuth and ellipticity of the polarization state of EMWs, can be expressed by the Stokes parameters (s_1, s_2, s_3) normalized by s_0, providing a quantitative way to specify the polarization state of EWMs [39–43]. There are four quantities in the Stokes parameters of EMWs, which can be calculated as follows [39]

$$\begin{cases} s_0 = E_x^2 + E_y^2 \\ s_1 = E_x^2 - E_y^2 \\ s_2 = 2E_xE_y\cos\Delta \\ s_3 = 2E_xE_y\sin\Delta \end{cases}, \tag{7}$$

Optics EXPRESS

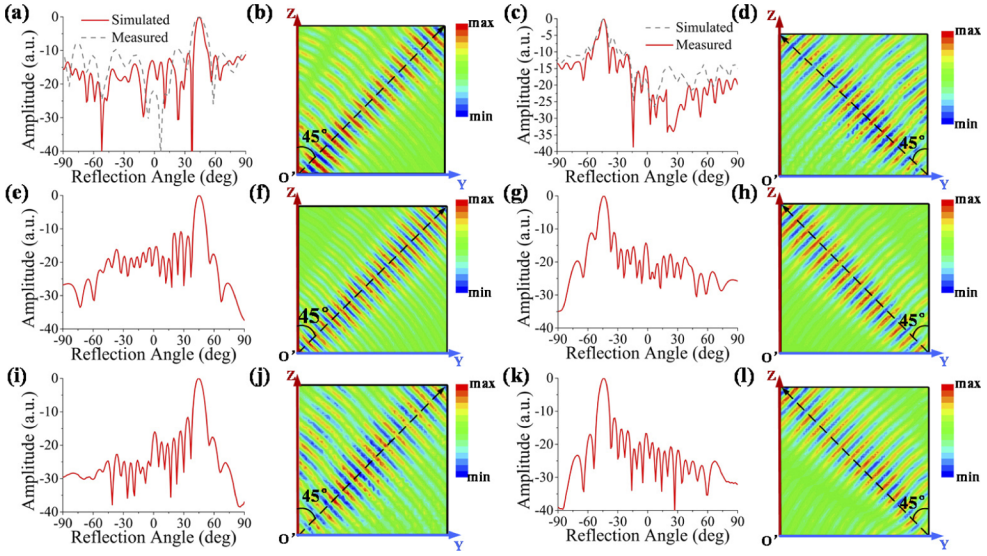

Fig. 4. Simulated and measured far-field radiation patterns and electric-field distributions in the YOZ plane of the three PBSMs at 5.8GHz. (a, e, i) Far-field radiation patterns in the YOZ plane for the PBSM #1, #2 and #3, respectively, under the illumination of $|\kappa_i^+\rangle (i = 1, 2, 3)$ correspondingly. (b, f, j) Electric-field distributions in the YO'Z plane corresponding to (a, e, i). (c, g, k) Far-field radiation patterns in the YOZ plane for the PBSM #1, #2 and #3, respectively, under the illumination of $|\kappa_i^-\rangle (i = 1, 2, 3)$ correspondingly. (d, h, l) Electric-field distributions in the YO'Z plane corresponding to (c, g, k).

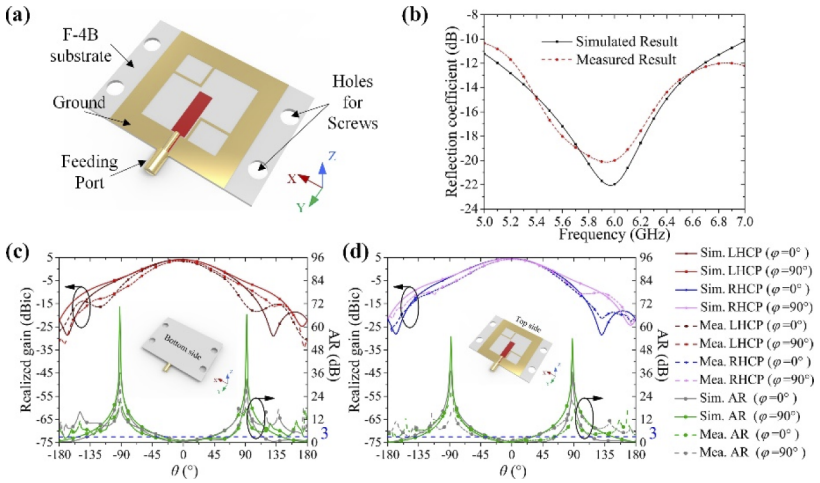

Fig. 5. (a) The geometry of the patch antenna. The simulated and measured reflection coefficients (b), realized gains, and axial ratios (c, d) for patch antenna with different setups.

Optics EXPRESS

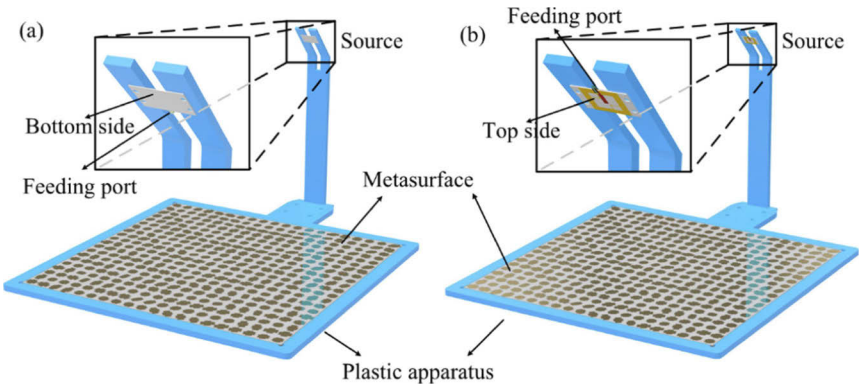

Fig. 6. The setup of the patch antenna to produce LCP (a) and RCP EMWs (b).

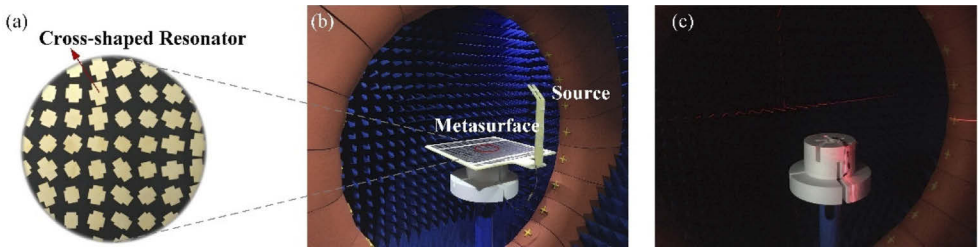

Fig. 7. (a) Photograph of the fabricated prototype. Experiment setup of proposed metasurfaces (b) and the patch antenna (c).

where E_x and E_y are the intensity of a pair of orthogonal components of EMWs along x- and y-directions; and Δ denotes the phase difference between the components of EMWs along x- and y-directions. Figure 8 shows the theoretical and simulated polarization states of the reflectance of three PBSMs in terms of Stokes parameters (s_1, s_2, s_3) normalized by s_0. The discrepancy between the simulated and theoretical Stokes parameters results from the different reflective amplitudes of each meta-atom for x- and y-polarized EMWs. Nevertheless, the simulated results matched the theoretical ones on the whole, proving that the proposed single-layer PBSMs perform well in independent manipulation of both circularly and elliptically polarized EMWs.

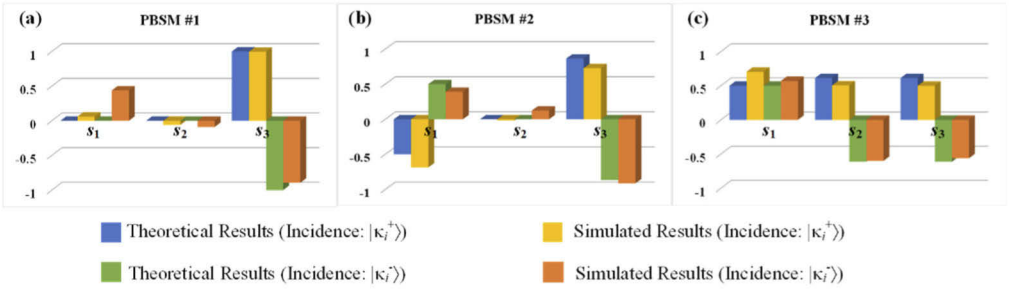

Fig. 8. Theoretical and simulated polarization state of the reflectance of (a) PBSM #1, (b) PBSM #2 and (c) PBSM #3 in terms of Stokes parameters

Optics EXPRESS

3.3. Orbital angular momentum multiplexor

In addition to PBSMs, three OAM multiplexors (OAMMs) are designed via the polarization-decoupled phase for arbitrary orthogonal circularly and elliptically polarized EMWs according to Eq. (5). Figure 9 is the conceptual schematic diagram of the proposed OAMMs, which are expected to manipulate a pair of orthogonal circularly or elliptically polarized EMWs independently. Similarly, three pairs of EMWs specified by $|\kappa_1^{\pm}\rangle$ (ω_1=π/4,ϕ_1=π/2), $|\kappa_2^{\pm}\rangle$ (ω_2=π/3,ϕ_2=π/2) and $|\kappa_3^{\pm}\rangle$ (ω_3=π/3,ϕ_3=π/4), respectively, are employed to illuminate three OAMMs, namely OAMM #1, #2 and #3, respectively. By appropriately employing the dynamical and the quasi-geometric phases in tandem, OAMMs can produce dual independent channels for multiplexing of OAM waves with different TCs, which are merged into a single beam. Assume that the TC of reflectance of $|\kappa_i^{+}\rangle (i = 1, 2, 3)$ is l_+=+1 while that of $|\kappa_i^{-}\rangle (i = 1, 2, 3)$ is l_-=−2 when the directions of the incident and the reflected EMWs are specified by unit vector $\overrightarrow{\mathrm{r_{iv}}} = (1, 0, 1)$ and $\overrightarrow{\mathrm{r_{rv}}} = (0, 0, 1)$, respectively, the phase profiles of the three OAMMs can be described as:

$$\varphi_{\pm}(x, y) = l_{\pm}\psi + k_0 \cdot (\vec{r}_{rv} \cdot \vec{r}_{xy} - \vec{r}_{iv} \cdot \vec{r}_{xy}) + \varphi_s(x, y), \tag{8}$$

where Ψ is the azimuthal angle. According to the Eqs. (5) and (8), the desired dynamical phase $\delta_x(x,y)$ and $\delta_y(x,y)$, as well as the quasi-geometric phase $\theta(x,y)$, can be given mathematically for the design of the three OAMMs.

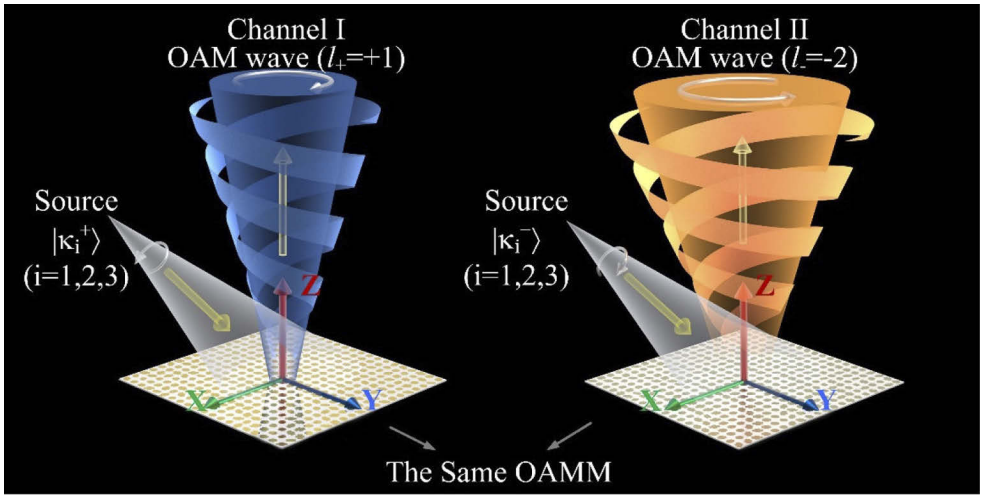

Fig. 9. Conceptual diagram of the proposed OAMMs. By means of the polarization-decoupled phase, the proposed OAMMs can create dual independent channels which are employed to transform incidence with orthogonal circular or elliptical polarization states into coaxial OAM waves with different TCs, realizing OAM multiplexing.

Figure 10 shows the simulated results of the anisotropic metasurfaces acting as OAMMs given by CST. It can be clearly observed that the performance of the three OAMMs is in accordance with expected results. Under the illumination of $|\kappa_i^{+}\rangle$ and $|\kappa_i^{-}\rangle (i = 1, 2, 3)$, a doughnut-shaped intensity with a singularity along the axial center and an anticlockwise spiral phase distribution can be identified on both the near- and far-field radiation patterns of OAMMs. More importantly, the radii of energy rings and corresponding phase distributions differ when the OAMMs are illuminated by incidence with different polarization states, confirming that OAM waves with polarization-dependent TC are produced. According to the corresponding phase distributions of the generated OAM waves, OAM waves with a TC of +1 are generated by the OAMMs under the illumination of $|\kappa_i^{+}\rangle (i = 1, 2, 3)$ while those with a TC of −2 are produced when the incidence is

Optics EXPRESS

$|\kappa_i^-\rangle (i = 1, 2, 3)$. Moreover, both of the generated OAM waves are propagating in the direction specified by $\overrightarrow{r_{rv}} = (0, 0, 1)$, which is consistent with expected results. Due to the restriction of metasurface source, only the OAMM for independent manipulation of dual-circularly EMWs was fabricated and measured. The experimental setup of OAMM #1 is identical to that of PBSM#1. Figures 10(m)–10(p) show the measured intensity and phase profiles of the generated OAM waves in the far-field zone, which were measured in an anechoic chamber. The measured results are in excellent agreement with the simulated results despite some defects caused by the fabrication error and experimental setups.

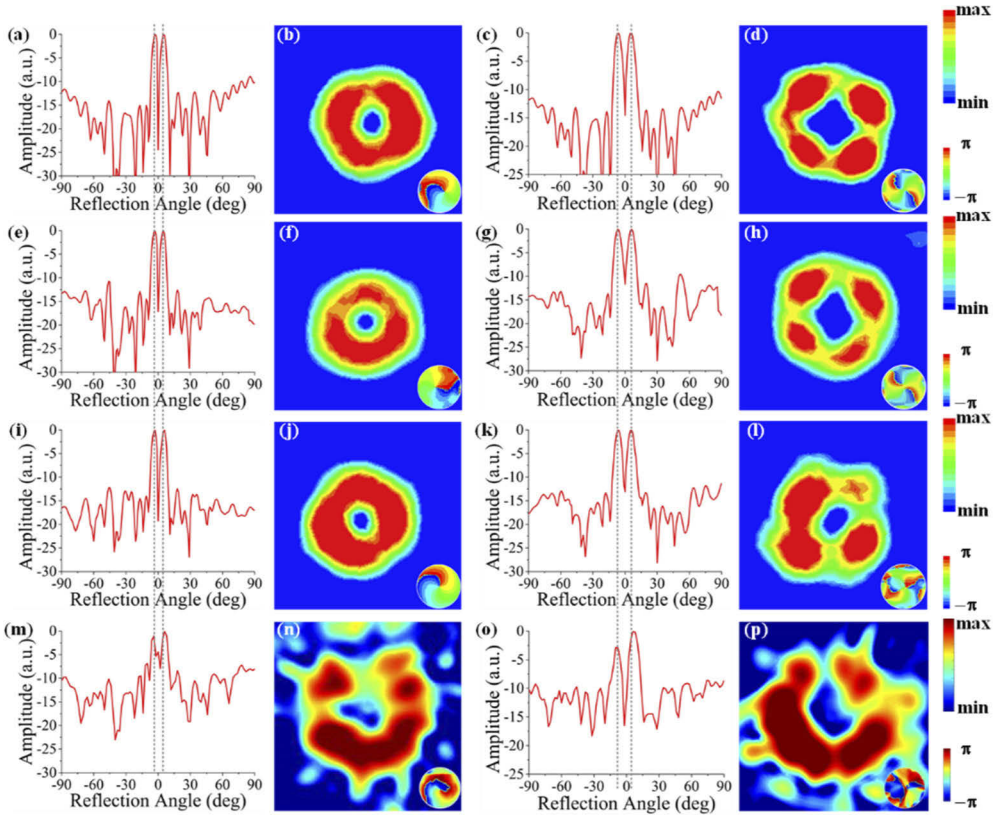

Fig. 10. Simulated and measured far-field radiation patterns, electric-field distributions and the corresponding phase distributions of the three OAMMs. Simulated far-field radiation patterns in the YOZ plane for (a) OAMM #1, (e) OAMM #2 and (i) OAMM #3 under the illumination of $|\kappa_i^+\rangle (i = 1, 2, 3)$. (b, f, j) Simulated electric-field distributions in the XOY plane corresponding to (a), (e) and (i), respectively. The insets show the simulated phase distribution in the corresponding XOY plane. Simulated far-field radiation patterns in the YOZ plane for (c) OAMM #1, (g) OAMM #2 and (k) OAMM #3 under the illumination of $|\kappa_i^-\rangle (i = 1, 2, 3)$. (d, h, l) Simulated electric-field distributions in the XOY plane corresponding to (c), (g) and (k), respectively. The insets show the simulated phase distribution in the corresponding XOY plane. The measured far-field radiation patterns of the fabricated prototype under the illumination of (m) LCP EMWs and (o) RCP EMWs. (n,p) The measured far-field electric field and phase distribution corresponding to (m) and (o), respectively.

Furthermore, the Stokes parameters of the generated OAM waves were studied to prove the efficiency of the proposed single-layer OAMMs. According to Eq. (7), the Stokes parameters can

Optics EXPRESS

be obtained, proving a quantitative method for studying the polarization state of the generated OAM waves. It can be easily found in Fig. 11 that the simulated results are in accordance with the designed ones, further verifying that the proposed single-layer anisotropic metasurface can effectively impose distinct phase profiles on an arbitrary set of orthogonal EMWs with circular or elliptical polarization states. The discrepancy between the simulated and theoretical Stokes parameters results from the different reflective amplitude of each meta-atom for x- and y-polarized EMWs.

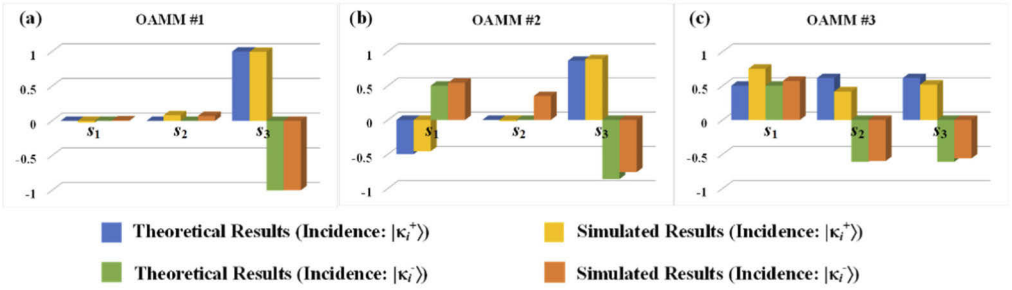

Fig. 11. The theoretical and simulated polarization state of the reflectance of (a) OAMM #1, (b) OAMM #2, and (c) OAMM #3 in terms of Stokes parameters

Additionally, the performance of OAMMs also demonstrates that the proposed designs can be used for spin-controlled OAM manipulation. Theoretically, OAM provides an unbounded degree of freedom which can create infinite independent channels for EMWs manipulation, engendering tremendously advanced applications ranging from optical micromanipulation to quantum optics [44]. Besides, spin angular momentum (SAM, also known as circular polarization) provides an additional degree of freedom for EMW manipulation. Hence, spin-controlled OAM waves have the advantage of doubling the number of independent channels that are achievable in linearly OAM waves-based communication systems. For this reason, the proposed designs can further enhance the channel capacity of a wireless communication system. For polarization-based multi-functional meta-devices, the proposed method has the advantage of doubling the achievable functionality of a single meta-device. Furthermore, the stringent requirement for perfect alignment of the polarization direction between transmitter and receiver can be ignored, as it does not cause performance degradation in communication systems when OAM waves carry SAM. As a result, the design complexity for OAM based communication systems can be reduced.

4. Conclusion

Single-layer metasurfaces are presented for independent manipulation of an arbitrary set of orthogonal EMWs with circular or elliptical polarization states. To impose arbitrary and independent phase profiles onto a set of orthogonal EMWs with arbitrary circular or elliptical polarization states, the metasurface are required to introduce the polarization-decoupled phase which is composed of the dynamical and the quasi-geometric phase based on the Jones matrix. Thus, meta-atoms with anisotropic resonances along two orthogonal directions were designed and employed in the proposed single-layer metasurfaces. In this way, the tandem employment of the dynamical and the quasi-geometric phases can be achieved by modifying the geometric shape and angular rotation of the meta-atoms. For proof-of-concept, three PBSMs and OAMMs operating in the microwave region are designed for independent manipulation of three sets of orthogonal EMWs with circular or elliptical polarization states. They all create dual polarization-dependent channels via the proposed tandem architecture, performing functions including polarization beam splitting and orbital OAM multiplexing excellently. Measured results are consistent with the simulated ones, confirming that the proposed single-layer reflective metasurfaces are

Optics EXPRESS

efficient devices that enable meta-devices to independently control arbitrary circular and elliptical polarized EMWs, achieving arbitrary functionalities.

Funding. Higher Education Discipline Innovation Project (111 Project B17007); Beijing Science and Technology Planning Project (No. Z191100002019015).

Acknowledgments. The authors thank Junlong Chen, Haoming Chen and Liangying Li from the Shenzhen University for their helpful suggestions and assistance in fabrication and experiments.

Disclosures. The authors declare no conflicts of interest.

References

1. J. Luan, S. Yang, D. Liu, and M. Zhang, "Polarization and direction-controlled asymmetric multifunctional metadevice for focusing, vortex and Bessel beam generation," Opt. Express **28**(3), 3732–3744 (2020).
2. X. Shan, L. Deng, Q. Dai, Z. Zhou, C. Liang, Z. Li, and G. Zheng, "Silicon-on-insulator based multifunctional metasurface with simultaneous polarization and geometric phase controls," Opt. Express **28**(18), 26359–26369 (2020).
3. J. Ji, S. Zhou, W. Wang, C. Luo, Y. Liu, F. Ling, and J. Yao, "Active multifunctional terahertz modulator based on plasmonic metasurface," Opt. Express **27**(3), 2363–2373 (2019).
4. J. S. Li and C. Zhou, "Multifunctional reflective dielectric metasurface in the terahertz region," Opt. Express **28**(15), 22679–22689 (2020).
5. N. Yu, P. Genevet, M. Kats, F. Aieta, J. Tetienne, F. Capasso, and Z. Gaburro, "Light Propagation with Phase Discontinuities: Generalized Laws of Reflection and Refraction," Science **334**(6054), 333–337 (2011).
6. Y. Guo, L. Yan, W. Pan, and B. Luo, "Achromatic polarization manipulation by dispersion management of anisotropic meta-mirror with dual-metasurface," Opt. Express **23**(21), 27566–27575 (2015).
7. N. Yu and F. Capasso, "Flat optics with designer metasurfaces," Nat. Mater. **13**(2), 139–150 (2014).
8. Q. Jiang, L. Cao, H. Zhang, and G. Jin, "Improve the quality of holographic image with complex-amplitude metasurface," Opt. Express **27**(23), 33700–33708 (2019).
9. N. Kou, S. Yu, and L. Li, "Generation of high-order Bessel vortex beam carrying orbital angular momentum using multilayer amplitude-phase-modulated surfaces in radiofrequency domain," Appl. Phys. Express **10**(1), 016701 (2017).
10. J. Du and J. Wang, "Dielectric metasurfaces enabling twisted light generation/detection/(de) multiplexing for data information transfer," Opt. Express **26**(10), 13183–13194 (2018).
11. Y. Tian, X. Jing, H. Yu, H. Gan, C. Li, and Z. Hong, "Manipulation of the arbitrary scattering angle based on all-dielectric transmissive Pancharatnam Berry phase coding metasurfaces in the visible range," Opt. Express **28**(21), 32107–32123 (2020).
12. Q. Guo, C. Schlickriede, D. Wang, H. Liu, Y. Xiang, T. Zentgraf, and S. Zhang, "Manipulation of vector beam polarization with geometric metasurfaces," Opt. Express **25**(13), 14300–14307 (2017).
13. Z. Zhang, J. Wang, R. Zhu, Y. Jia, T. Liu, M. Yan, J. Jiang, Y. Li, Y. Meng, and S. Qu, "Multifunctional full-space metasurface controlled by frequency, polarization and incidence angle," Opt. Express **29**(5), 7544–7557 (2021).
14. Q. He, S. Sun, S. Xiao, and L. Zhou, "High-efficiency metasurfaces: principles, realizations, and applications," Adv. Opt. Mater. **6**(19), 1800415 (2018).
15. Y. Yuan, K. Zhang, B. Ratni, Q. Song, X. Ding, Q. Wu, S. N. Burokur, and P. Genevet, "Independent phase modulation for quadruplex polarization channels enabled by chirality-assisted geometric-phase metasurfaces," Nat. Commun. **11**(1), 1–9 (2020).
16. W. T. Chen, K. Y. Yang, C. M. Wang, Y. W. Huang, G. Sun, I. D. Chiang, C. Y. Liao, W. L. Hsu, H. T. Lin, S. Sun, L. Zhou, A. Q. Liu, and D. P. Tsai, "High-efficiency broadband meta-hologram with polarization-controlled dual images," Nano Lett. **14**(1), 225–230 (2014).
17. H. X. Xu, S. Tang, X. Ling, W. Luo, and L. Zhou, "Flexible control of highly-directive emissions based on bifunctional metasurfaces with low polarization cross-talking," Ann. Phys. **529**(5), 1700045 (2017).
18. L. Deng, Y. Wu, C. Zhang, W. Hong, B. Peng, J. Zhu, and S. Li, "Manipulating of different-polarized reflected waves with graphene-based plasmonic metasurfaces in terahertz regime," Sci. Rep. **7**(1), 1–10 (2017).
19. G. Shang, H. Li, Z. Wang, K. Zhang, S. N. Burokur, J. Liu, Q. Wu, X. Ding, and X. Ding, "Coding metasurface holography with polarization-multiplexed functionality," J. Appl. Phys. **129**(3), 035304 (2021).
20. X. Chen, L. Huang, H. Mühlenbernd, G. Li, B. Bai, Q. Tan, G. Jin, C. W. Qiu, T. Zentgraf, and S. Zhang, "Reversible Three-Dimensional Focusing of Visible Light with Ultrathin Plasmonic Flat Lens," Adv. Opt. Mater. **1**(7), 517–521 (2013).
21. L. Deng, Y. Zhang, J. Zhu, and C. Zhang, "Wide-band circularly polarized reflectarrayusing graphene-based pancharatnam-berry phase unit-cells for terahertz communication," Materials **11**(6), 956 (2018).
22. H. Wang, Y. Li, Z. Yang, S. Sui, H. Chen, Y. Han, J. Wang, J. Zhang, and S. Qu, "Helicity-independent metasurface for versatile functionalities with shared aperture," Appl. Phys. Express **12**(8), 085501 (2019).
23. D. Lin, A. L. Holsteen, E. Maguid, P. Fan, P. G. Kik, E. Hasman, and M. L. Brongersma, "Polarization-independent metasurface lens employing the Pancharatnam-Berry phase," Opt. Express **26**(19), 24835–24842 (2018).

Optics EXPRESS

24. L. Tang, R. Jin, Y. Cao, J. Li, J. Wang, and Z. G. Dong, "Spin-dependent dual-wavelength multiplexing metalens," Opt. Lett. **45**(18), 5258–5261 (2020).
25. Y. Meng, Z. Liu, Z. Xie, R. Wang, T. Qi, F. Hu, H. Kim, Q. Xiao, X. Fu, Q. Wu, S. Bae, M. Gong, and X. Yuan, "Versatile on-chip light coupling and (de) multiplexing from arbitrary polarizations to controlled waveguide modes using an integrated dielectric metasurface," Photonics Res. **8**(4), 564–576 (2020).
26. A. Arbabi, Y. Horie, M. Bagheri, and A. Faraon, "Dielectric metasurfaces for complete control of phase and polarization with subwavelength spatial resolution and high transmission," Nat. Nanotechnol. **10**(11), 937–943 (2015).
27. Y. Meng, F. Hu, Z. Liu, P. Xie, Y. Shen, Q. Xiao, X. Fu, S. Bae, and M. Gong, "Chip-integrated metasurface for versatile and multi-wavelength control of light couplings with independent phase and arbitrary polarization," Opt. Express **27**(12), 16425–16439 (2019).
28. Y. Yuan, K. Zhang, X. Ding, B. Ratni, S. N. Burokur, and Q. Wu, "Complementary transmissive ultra-thin meta-deflectors for broadband polarization-independent refractions in the microwave region," Photonics Res. **7**(1), 80–88 (2019).
29. R. C. Devlin, A. Ambrosio, N. A. Rubin, J. B. Mueller, and F. Capasso, "Arbitrary spin-to–orbital angular momentum conversion of light," Science **358**(6365), 896–901 (2017).
30. K. Zhang, Y. Yuan, X. Ding, B. Ratni, S. N. Burokur, and Q. Wu, "High-efficiency metalenses with switchable functionalities in microwave region," ACS Appl. Mater. Interfaces **11**(31), 28423–28430 (2019).
31. J. B. Mueller, N. A. Rubin, R. C. Devlin, B. Groever, and F. Capasso, "Metasurface polarization optics: independent phase control of arbitrary orthogonal states of polarization," Phys. Rev. Lett. **118**(11), 113901 (2017).
32. H. X. Xu, L. Han, Y. Li, Y. Sun, J. Zhao, S. Zhang, and C. W. Qiu, "Completely spin-decoupled dual-phase hybrid metasurfaces for arbitrary wavefront control," ACS Photonics **6**(1), 211–220 (2019).
33. R. Barakat, "Jones matrix equivalence theorems for polarization theory," Eur. J. Phys. **19**(3), 209–216 (1998).
34. B. L. Van Der Waerden, "*Group theory and quantum mechanics (Vol. 214)*," Springer Science & Business Media 214(2012).
35. S. Sun, Q. He, J. Hao, S. Xiao, and L. Zhou, "Electromagnetic metasurfaces: physics and applications," Adv. Opt. Photonics **11**(2), 380–479 (2019).
36. L. Yan, W. Zhu, M. F. Karim, H. Cai, A. Y. Gu, Z. Shen, P. Chong, D. Tsai, and A. Q. Liu, "Arbitrary and independent polarization control in situ via a single metasurface," Adv. Opt. Mater. **6**(21), 1800728 (2018).
37. E. Collett and B. Schaefer, "Visualization and calculation of polarized light. I. The polarization ellipse, the Poincare sphere and the hybrid polarization sphere," Appl. Opt. **47**(22), 4009–4016 (2008).
38. A. Singh, "Stokes vector-based polarization management in optical communication system: a review," Opt. Eng. **59**(09), 090901 (2020).
39. M. J. Walker, "Matrix calculus and the Stokes parameters of polarized radiation," Am. J. Phys. **22**(4), 170–174 (1954).
40. W. H. McMaster, "Polarization and the Stokes parameters," Am. J. Phys. **22**(6), 351–362 (1954).
41. H. G. Berry, G. Gabrielse, and A. E. Livingston, "Measurement of the Stokes parameters of light," Appl. Opt. **16**(12), 3200–3205 (1977).
42. W. M. Boerner, M. El-Arini, C. Y. Chan, and P. Mastoris, "Polarization dependence in electromagnetic inverse problems," IEEE Trans. Antennas Propag. **29**(2), 262–271 (1981).
43. D. I. Nagirner, "Constraints on matrices transforming Stokes vectors," Astron. Astrophys. **275**, 318 (1993).
44. Y. Shen, X. Wang, Z. Xie, C. Min, X. Fu, Q. Liu, M. Gong, and X. Yuan, "Optical vortices 30 years on: OAM manipulation from topological charge to multiple singularities," Light: Sci. Appl. **8**(1), 90 (2019).